A NEW CALCULATION METHOD FOR THE CHARACTERISTIC IMPEDANCE OF TRANSMISSION LINES WITH MODIFIED GROUND STRUCTURES OR PERTURBATION

J. Lim, J. Lee, J. Lee, S.-M. Han, and D. Ahn

Department of Electrical and Communication Engineering
Soonchunhyang University
646, Eupnaeri, Shinchang, Asan
Chungnam 336-745, R.O.Korea

Y. Jeong

Division of Electronics and Information Engineering
Chonbuk National University
664-14, Deokjin-dong, Deokjin-gu, Jeonju
Chonbuk 561-756, R.O.Korea

Abstract—In this paper, a new calculating method for the characteristic impedance (Z_c) of transmission lines with perturbation and periodic modified ground structure (MGS), such as defected ground structure (DGS), photonic bandgap (PBG), and substrate integrated artificial dielectric (SIAD), is discussed. The proposed method is based on simple transmission line theories and proper related equations. The previous method to find Z_c of transmission lines with MGS or perturbation produces the fluctuating Z_c value depending on frequency, while the proposed method results in a constant value without frequency-dependence. As examples, several microstrip lines with DGS, PBG, and SIAD structure are simulated and measured, and their Z_c values are calculated from S-parameters by the previous and proposed methods. It is shown that the Z_c obtained by the proposed method is much more reliable than that calculated by the previous method for all examples.

1. INTRODUCTION

Many electromagnetic circuits are implemented with the form of transmission line structures based on planar printed circuit boards (PCBs), which are composed of a dielectric material layer and ground/signal metal planes. One of the most widely used transmission lines for high frequency circuits is microstrip line. A microstrip line consists of a dielectric substrate covered by metal layers on both sides, one of which is patterned for signal line, the other one for the ground plane.
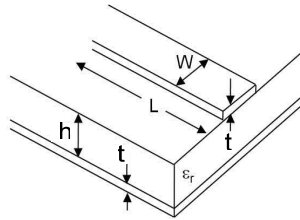
Figure 1. Structure of a standard microstrip line.

As illustrated in Figure 1, when the thickness and dielectric constant of the substrate are "h" and "ε_r", respectively, the line width ("W") and length ("L") of the microstrip line correspond to a specified characteristic impedance ("Z_c") and electrical length ("θ") at a specified frequency [1]. Here "t" is the thickness of metal layers. Normally the thickness is not a critical factor in determining Z_c.

The dimension of W corresponding to a specified Z_c is directly dependent on the effective dielectric constant ("ε_{eff}") which is also strongly related to ε_r [1]. Normally the effective dielectric constant of microstrip lines is fixed under the given W, H, and ε_r. In other words, a pair of W and Z_c exists for the given substrate with h, t, and ε_r.

Recently, microstrip transmission lines combined by perturbation or modified ground structures (MGS) such as defected ground structure (DGS), photonic bandgap (PBG), and substrate integrated artificial dielectric (SIAD) structures have been proposed and studied popularly [2–6]. In addition, those structures have been widely applied to high frequency circuits such as filters, dividers, couplers, mixers, amplifiers, multipliers, baluns, and antennas [7–25].

In order for those transmission line elements with perturbation or MGS to be applied to high frequency circuits, the consideration for the deviation of characteristic impedance should be carefully taken into. Theoretically and practically, it is well known that all high frequency circuits should have proper design equations and

matching performances based on the accurate characteristic impedance of transmission line elements. In the previous works mentioned above, the accurate characteristic impedance-based circuit applications have been one of major research topics [6, 11, 12, 19]. Therefore it is quite important to calculate accurately the deviation of the characteristic impedance of transmission lines due to any MGS, perturbation, and arbitrary periodicity in the point of view of circuit applications as well as the transmission line itself.

It is well known that modified transmission lines (MTL) — transmission lines with a perturbation such as periodicity or modified dielectric and ground structures — have some modification in the electrical length, slow wave factor (SWF), characteristic impedance (Z_c), and effective dielectric constant from the typical values [2–6].

In this work, a new calculation method for characteristic impedance of MTLs will be described. The proposed method is based on the well known reflection and transmission theories of transmission lines. The obtained characteristic impedances using the proposed method are almost constant and independent of frequency, while the conventional method results in the frequency-dependent Z_c. The perturbation and MGSs combined to regular microstrip lines include DGS, PBG, and SIAD structure in this work. The microstrip line will be mentioned as the representative transmission line.

2. MODIFIED TRANSMISSION LINE STRUCTURES

The purpose of this work is not to describe the physical structures and electrical characteristics of microstrip lines with DGS, PBG, and SIAD "for the first time". In practice, those have been already discussed well in the previous works by Radisic, Kim, Yun, Coulombe et al. [3–6]. On the contrary, it is the aim of this work to propose a new method to calculate the characteristic impedance of those MTLs. However, it would be helpful for better understanding the proposed method to introduce briefly microstrip lines with DGS, PBG, and SIAD.

2.1. Photonic Bandgap Structures (PBG)

One of popular periodic structures for high frequency planar transmission lines is two-dimensional photonic bandgap (PBG). A popular PBG structure for microwave application is realized by etching the ground metal plane or constructing the dielectric-holes around the signal line infinitely and periodically [3, 17]. Figure 2 shows the representative PBG structure for planar microstrip line proposed by Radisic et al. [3, 17]. The advantage of microstrip lines with PBG is
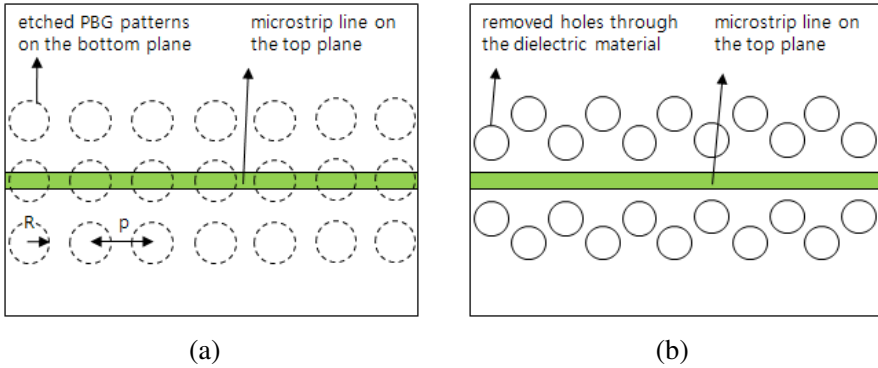
Figure 2. Planar PBG structural microstrip line (a) with ground metal removed periodically on the bottom ground plane, and (b) with dielectric layer removed.
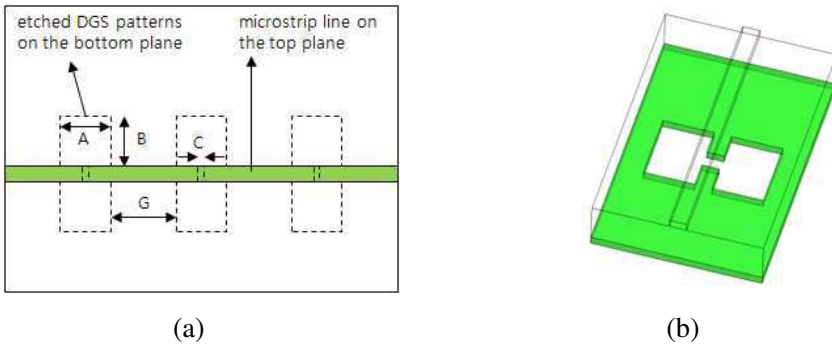
Figure 3. Microstrip line with DGS structure: (a) layout and (b) 3-D view.

the increased SWF, which can be used for size reduction of microwave circuits.

2.2. Defected Ground Structures (DGS)

Typical DGS shape is just like a dumb-bell shown in Figure 3, which is realized by etching defected areas on the ground plane and a connecting slot between defected rectangles. Although the number of DGS patterns is less than that of the periodic PBG, it is considered as a kind of periodic structure for microstrip line. The equivalent circuit of DGS consists of the additional inductance and capacitance, and the equivalent inductance is dominant over the capacitance. It is much easier to establish the equivalent circuit because the transmission,

reflection, and suppression characteristics of DGS microstrip line are very clear and definite. Furthermore, DGS has prominent advantages of being applied to microwave circuits such as filters, dividers, couplers, amplifiers, and so on [7, 9–20].

2.3. Substrate Integrated Artificial Dielectric (SIAD) Structures

Figure 4 shows the microstrip line with SIAD structures proposed recently [6]. There are two dielectric layers with the same or different dielectric constant. The microstrip signal line is placed on the uppermost plane, and the wide ground plane exists on the undermost plane. There are a lot of metalized periodical via-holes through the second dielectric layer. No metal plane exists between two dielectric layers. Dimensions of "h_1", "h_2", "d", and "p" in Figure 4 are the thickness of the first and second layers, diameter of via-holes, and length of the periodicity, respectively.

(a)   (b)
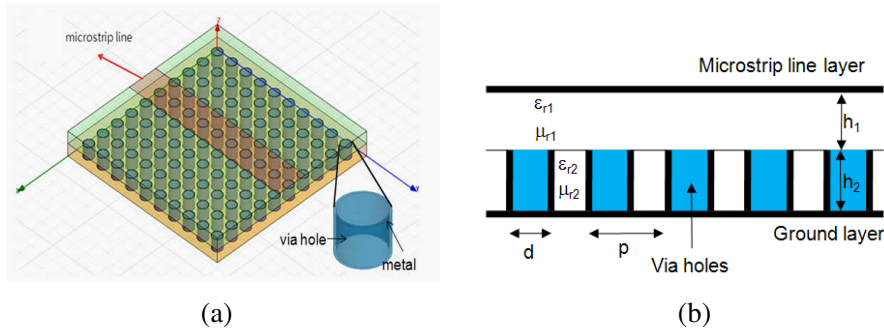
Figure 4. SIAD structure and transmission line: (a) 3-D view and (b) side view.

The representative effect of the microstrip with SIAD is the increased effective permittivity due to the increased capacitance between signal trace and via-hole tops, and between via-holes compared to regular microstrip lines. In addition, the effective permeability also increases because of the increased ratio between total magnetic flux and current from the regular microstrip line. The increase of the effective permittivity (ε_{eff}) is dominant over the effective permeability (μ_{eff}), so the characteristic impedance is reduced from regular microstrip lines [6]. So when a low impedance transmission line is required, SIAD microstrip line is expected to be a good solution.

One of advantages of SIAD microstrip line is the increase of the effective refractive index (η_{eff}) which is expressed by the square root of the multiplication of effective permittivity and permeability [6]. It is noted that the effective refractive index value strongly depends on the Z_c. So, it is very important to calculate the characteristic impedance exactly in advance for applications.

It is noted that the characteristic impedance of microstrip lines with MGS or perturbation is not maintained any more from that of the typical microstrip lines. The same situation goes for all types of periodic structures combined to other transmission lines. The deviation of Z_c is caused by the additional inductive and capacitive elements due to the MGS or perturbation. So it is important to calculate the Z_c exactly because its characteristic impedance becomes a critical factor for design when microstrip line elements are applied to high frequency circuits.

The increased electrical length of the microstrip lines with MGS or perturbation should be discussed. As for DGS, the equivalent inductance per unit length of the microstrip line increases due to DGS, so the electrical length is no longer the same as the original one. This means the slow-wave effect gets stronger in the microstrip line with DGS. The same phenomenon occurs for other types of MGS or perturbation.

An attention should be paid to the new Z_c and the SWF because the microstrip line with MGS or perturbation has longer electrical length than the typical microstrip line with the same physical length. Therefore, the original physical length might be shortened by inserting MGS or perturbation in order to maintain the same electrical length. This is a very useful clue for application to size-reduced high frequency circuits.
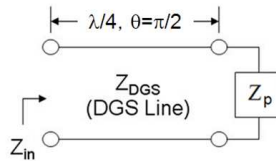
3. CALCULATION OF THE CHARACTERISTIC IMPEDANCES

3.1. Previous Method Using $\lambda/4$ Transmission Line Model

The method to calculate the characteristic impedance of transmission lines with DGS has been studied previously [11, 12]. In the previous work, the equivalent $\lambda/4$ transmission line model is established first, and the magnitude of reflection coefficient ($|\Gamma|$) and S_{11} are related at the frequency where S_{11} shows its maximum value. At this frequency, $|\Gamma|$ is related to the input impedance.

Figure 5 and Figure 6 show an example of microstrip line with DGS and its S-parameters, and the equivalent $\lambda/4$ transmission line model, respectively. At about 2.6 GHz, the maximum value of S_{11}
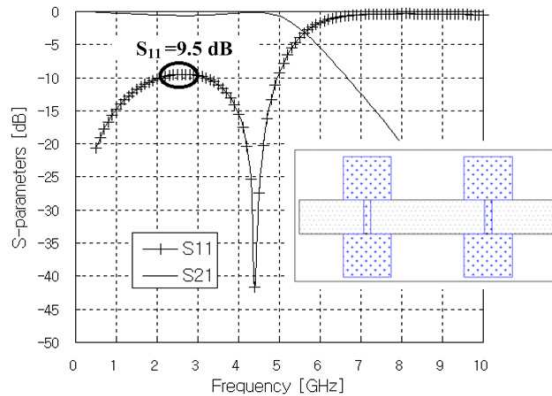
Figure 5. Example of DGS microstrip line and its S-parameters.

Figure 6. Equivalent $\lambda/4$ transmission line model to calculate the characteristic impedance of DGS microstrip line.

is $-9.5\,\text{dB}$. It is easily understood that the microstrip in Figure 5 is just like a quarter-wavelength transmission line at $2.6\,\text{GHz}$. So if this transmission line is terminated by the reference impedance (port impedance Z_p, normally $50\,\Omega$), the unknown characteristic impedance (Z_{DGS}) is determined easily using (1)–(3).

$$S_{11}\,[\text{dB}] = 20\log|\Gamma| \tag{1}$$

$$Z_{in} = Z_p\frac{1+|\Gamma|}{1-|\Gamma|} \tag{2}$$

$$Z_{DGS} = \sqrt{Z_{in}Z_p} = Z_p\sqrt{\frac{1+|\Gamma|}{1-|\Gamma|}} \tag{3}$$

However, a serious drawback exists in the previous method. The calculated characteristic impedance is acceptable only at the frequency where the effective electrical length is $\lambda/4$. It is noted that Z_{in} is always real value from (2). However the input impedance is a real value only at the frequency where the electrical length is $\lambda/4$. If one calculates the characteristic impedance using the S-parameters shown in Figure 5
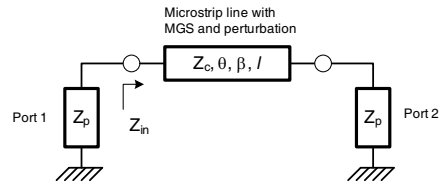
and (1)–(3), the resultant Z_{DGS} fluctuates depending on the frequency. This means that the calculated Z_{DGS} at other frequencies is not correct any more.

(a)   (b)
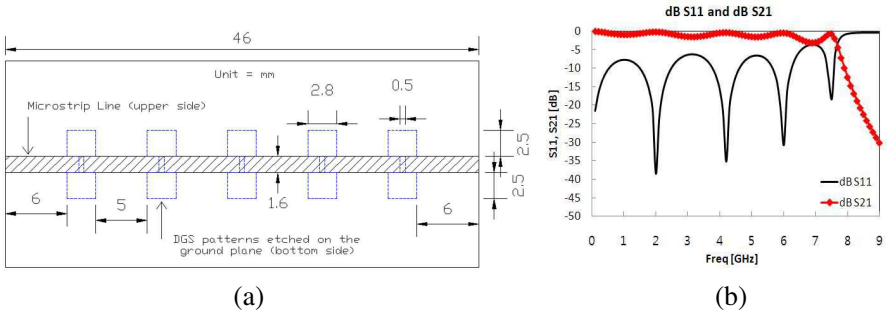
Figure 7. Microstrip line with DGS patterns: (a) layout and (b) S-parameters.
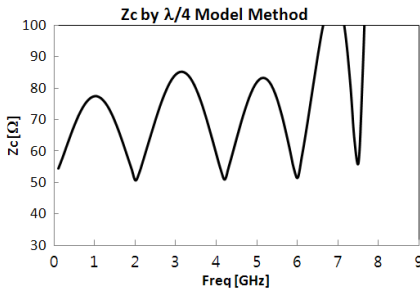
Figure 8. Calculated character-istic impedance using the equiva-lent $\lambda/4$ transmission line model.

Figure 9. Diagram for finding the characteristic impedance us-ing the proposed method.

Figure 7 shows the example of a microstrip line with 5 DGS patterns and its S-parameters when the dielectric constant and thickness of the substrate are 2.2 and 31 mils, respectively. Figure 8 shows that the calculated characteristic impedance fluctuates depending on the frequency.

3.2. The Proposed Analytic Method

Figure 9 shows the equivalent diagram for the proposed method to calculate the characteristic impedance of transmission lines with MGS or perturbation. According to the basic transmission line theories, the electrical length (θ) is the product of phase constant (β) and line length

(l). Z_p is the terminating impedance at in/output ports, and that is normally $50\,\Omega$ in practice. The input impedance (Z_{in}) is expressed and related to S_{11} as shown in (4) and (5). The real and imaginary parts of S_{11} can be separated, and Z_c and Z_{in} can be normalized to Z_p like (6a) and (6b).

Relating and developing further $(4), (5), (6a)$, and $(6b)$, one obtains (7) easily. It is clear that the real and imaginary parts of (7) should be zero, so two equations of the second degree are resulted as depicted in (8a) and (8b). These equations have the typical form of the quadratic equation "$aX^2 + bX + c = 0$". For the convenience, we are going to describe, hereinafter, using the basic equation form of "$aX^2 + bX + c = 0$".

$$Z_{in} = Z_c \frac{Z_p + jZ_c \tan\theta}{Z_c + jZ_p \tan\theta} \tag{4}$$

$$S_{11} = \frac{Z_{in} - Z_p}{Z_{in} + Z_p} = \frac{z_{in} - 1}{z_{in} + 1} = Re\,(S_{11}) + jIm\,(S_{11}) \equiv rs_{11} + jis_{11} \tag{5}$$

$$z_{in} = \frac{Z_{in}}{Z_p} = \frac{Z_c}{Z_p} \frac{1 + j\frac{Z_c}{Z_p}\tan\theta}{\frac{Z_c}{Z_p} + j\tan\theta} = z_c \frac{1 + jz_c \tan\theta}{z_c + j\tan\theta} \tag{6a}$$

$$z_c = \frac{Z_c}{Z_p} \tag{6b}$$

$$2z_c rs_{11} - \left(z_c^2 + 1\right)\tan\theta\, is_{11}$$
$$+ j\left[2z_c\, is_{11} + \left(z_c^2 + 1\right)\tan\theta\, rs_{11} - \left(z_c^2 - 1\right)\tan\theta\right] = 0 \tag{7}$$

$$z_c^2 - \frac{2rs_{11}}{\tan\theta\, is_{11}} z_c + 1 = 0 \tag{8a}$$

$$z_c^2 + \frac{2is_{11}}{\tan\theta\,(rs_{11} - 1)} z_c - \frac{1 + rs_{11}}{1 - rs_{11}} = 0 \tag{8b}$$

In (8a), the determinant, $D(= b^2 - 4ac)$, may be positive or negative depending on the magnitude of b because $a = c = 1$. If the determinant is a negative value, the solutions are meaningless. However, Z_c should be real because it is the characteristic impedance of the transmission line in Figure 9. It is also noted that the magnitude of rs_{11} and is_{11} are less than 1 because the transmission line is a passive element. Therefore it is of no use to calculate z_c using (8a) in some cases.

Taking a deep consideration into (8b), "$(1 + rs_{11})/(1 - rs_{11})$" is always positive because the magnitude of rs_{11} is less than 1, then c of "$aX^2 + bX + c = 0$" is always negative. One can easily find that the

determinant is always positive and there exist two real roots of (8b). Out of two z_c values, one is the proper solution and selected, while the other is not a right solution and dismissed.

It should be noted that θ is limited within 90° or between 90° and 180° for (8b) to be applied in finding z_c because i) $\tan\theta$ approaches to infinity (∞) when θ approaches to 90°, and ii) a singularity problem occurs when θ approaches to 180°. In addition, if θ is equal to 90° which corresponds to $\lambda/4$, Figure 9 represents the perfect quarter-wavelength transformer matching condition, and (3) is valid only at the frequency where the line length is $\lambda/4$. If the line length is longer than $\lambda/2$, (8b) may produce solutions which are somewhat meaningless or repeated ones. Relying on experiences, the calculated characteristic impedance is almost constant and reliable at the frequency range when the line length is between $\lambda/8$ and $3\lambda/8$. When the line length is near 0 or $\lambda/2$, θ and S_{11} change radically, and this makes the characteristic impedance unstable, which would be dismissed.
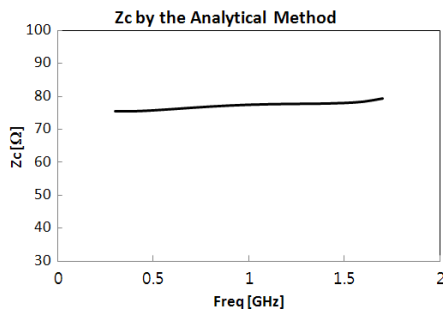
4. APPLICATIONS OF THE PROPOSED METHOD TO MTLS
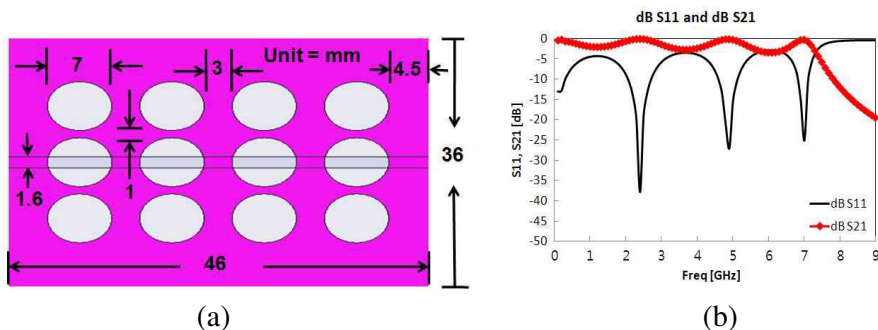
4.1. DGS Microstrip Lines

The proposed method has been applied to find the characteristic impedance of the microstrip line with DGS. Figure 10 shows the fabricated circuit which is exactly the same as Figure 7(a). The measured S-parameters are so similar to the results in Figure 7(b), so it is not shown here. It is estimated that the electrical length is near the quarter-wave at around 1 GHz from Figure 7(b) and its S_{21} phase which is not shown. Figure 11 shows the calculated characteristic impedance, which is quite different from the results shown in Figure 8 except at about 1 GHz. The frequency-dependence of characteristic impedance has been quite mitigated in Figure 11, while it is strong in Figure 8.

Figure 10. Fabricated microstrip line with DGS.

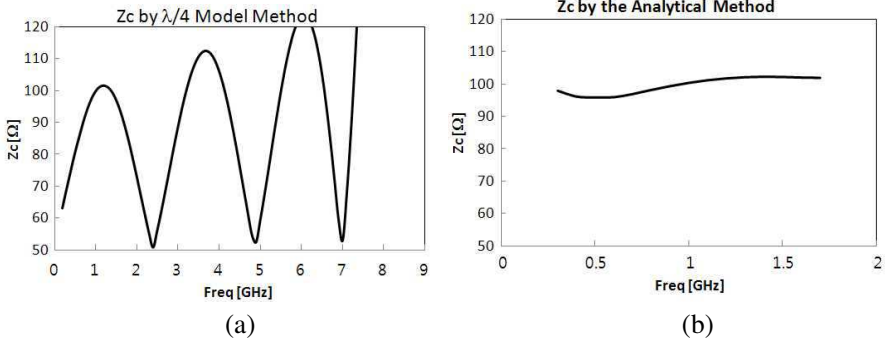**Figure 11.** Calculated characteristic impedance of the microstrip line with DGS using the proposed method.

(a)	(b)

**Figure 12.** Microstrip line with PBG patterns: (a) layout and (b) simulated S-parameters.

Figure 13. Fabricated microstrip line with PBG.

4.2. PBG Microstrip Lines

The proposed method has been applied to the microstrip line with PBG. Figure 12(a) and Figure 12(b) depict the layout of the microstrip line with PBG and its simulated S-parameter characteristics, and Figure 13 shows the photograph of the fabricated one. For the same reason, the measured S-parameters are not shown here. Figure 14(a) and Figure 14(b) show the characteristic impedances based on the

(a)   (b)

Figure 14. Calculated characteristic impedance of the microstrip line with PBG using (a) the previous $\lambda/4$ model method and (b) the proposed method.


(a)   (b)
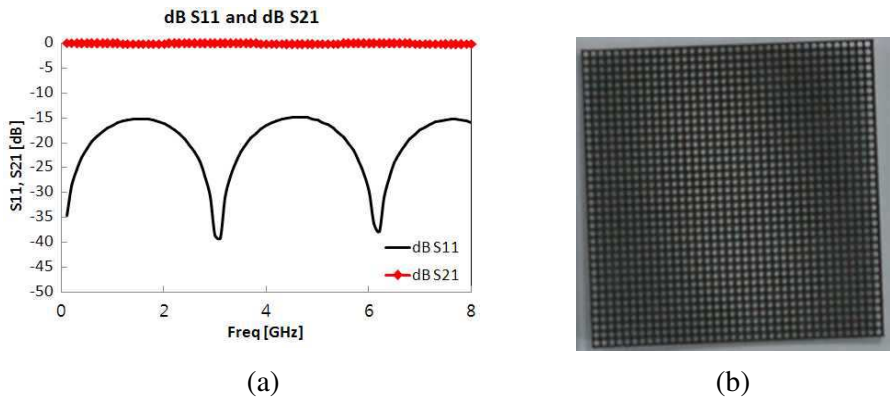
Figure 15. SIAD microstrip transmission line: (a) S-parameters and (b) photograph of the second substrate with a lot of via-holes.

previous and proposed methods, respectively. The difference between two results is evident. The same substrate of which dielectric constant and thickness are 2.2 and 31 mils has been adopted for the PBG microstrip line.

4.3. SIAD Microstrip Lines

Now the proposed method has been applied to find the characteristic impedance of the microstrip line with SIAD. Figure 15(a) and Figure 15(b) show the S-parameters and fabricated SIAD substrate with a lot of via-holes. The thicknesses of two substrates and dielectric
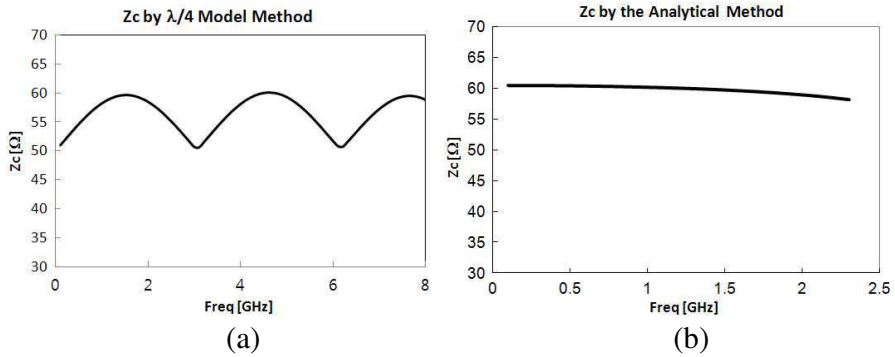
Figure 16. Characteristic impedances of the SIAD microstrip transmission line using (a) previous method and (b) proposed method.

constant are 5 mils ($= h_1$), 31 mils ($= h_2$), and 2.2, respectively. The diameter of via-holes and periodicity are 0.8 mm and 1.3 mm, and line width is 0.91 mm. The electrical length is near the quarter-wavelength at 1.7 GHz from Figure 15(a) and its S_{21} phase which is not shown. Figure 16(a) and Figure 16(b) show the calculated characteristic impedances by the previous and proposed methods, respectively. The characteristic impedance by the equivalent $\lambda/4$ transmission line model does not converge, but fluctuates depending on the frequency. So the average value has been selected as the representative characteristic impedance in the early study [6]. However, the proposed method shows the characteristic impedance which is almost constant regardless of frequency.

5. CONCLUSION

An analytic method to calculate the characteristic impedance of transmission lines with modified ground structures or perturbation has been discussed. The proposed method utilizes the S-parameters and basic transmission line theories. The proposed method results in the almost constant value without frequency-dependence, while the previous method which utilizes the equivalent $\lambda/4$ transmission line model produces the characteristic impedances with serious fluctuation depending on frequency.

In order to verify the proposed method, three types of microstrip line with DGS, PBG, and SIAD have been simulated, fabricated and measured. The obtained characteristic impedances by the proposed method were constant values without frequency-dependency.

It is expected that the proposed method can be applied to all kinds of transmission line with other types of modified ground structure or perturbation. In addition, the proposed method is believed to play a good role in determining the new characteristic impedance or deviation from typical transmission lines. It is so essential and important to get the accurate characteristic impedance of transmission line elements for successful applications in design of high frequency circuits and antennas.

REFERENCES

1. Gupta, K. C., et al., *Microstrip Lines and Slotlines*, 2nd edition, Artech House, Boston, 1996.
2. Gupta, S. K. and K. J. Vinoy, "A compact defected ground microstrip device with photonic bandgap effects," *Journal of Electromagnetic Waves and Applications*, Vol. 23, No. 2–3, 255–256, 2009.
3. Radisic, V., Y. Qian, R. Coccioli, and T. Itoh, "Novel 2-D photonic bandgap structure for microstrip lines," *IEEE Microw. Guide Wave Lett.*, Vol. 8, No. 2, 69–71, Feb. 1998.
4. Yun, T. Y. and K. Chang, "Uniplanar one-dimensional photonic-bandgap structures and resonators," *IEEE Trans. Microwave Theory Tech.*, Vol. 49, No. 3, 549–553, Mar. 2001.
5. Kim, C. S., J. S. Park, D. Ahn, and J. B. Lim, "A novel 1-D periodic defected ground structure for planar circuits," *IEEE Microw. Guide Wave Lett.*, Vol. 10, No. 4, 131–133, Apr. 2000.
6. Coulombe, M., H. V. Nguyen, and C. Caloz, "Substrate integrated artificial dielectric (SIAD) structure for miniaturized microstrip circuits," *IEEE. Ant. and Wir. Prop. Lett.*, Vol. 6, 575–579, Dec. 2007.
7. Chen, X.-Q., R. Li, S.-J. Shi, Q. Wang, L. Xu, and X.-W. Shi, "A novel low pass filter using elliptic shape defected ground structure," *Progress In Electromagnetics Research B*, Vol. 9, 117–126, 2008.
8. Weng, L. H., Y.-C. Guo, X.-W. Shi, and X.-Q. Chen, "An overview on defected ground structure," *Progress In Electromagnetics Research B*, Vol. 7, 173–189, 2008.
9. Mohra, A. S. S., "Compact lowpass filter with sharp transition band based on defected ground structures," *Progress In Electromagnetics Research Letters*, Vol. 8, 83–92, 2009.
10. Lim, J. S., C. S. Kim, D. Ahn, Y. C. Jeong, and S. Nam, "Design

of low-pass filters using defected ground structure," *IEEE Trans. Microwave Theory Tech.*, Vol. 53, No. 8, 2539–2545, Aug. 2005.

11. Lim, J. S., S. W. Lee, C. S. Kim, J. S. Park, D. Ahn, and S. Nam, "A 4 : 1 unequal wilkinson power divider," *IEEE Microw. Wireless Compon. Lett.*, Vol. 11, No. 3, 124–126, Mar. 2001.

12. Lim, J. S., C. S. Kim, J. S. Park, D. Ahn, and S. Nam, "Design of 10 dB 90° branch line coupler using microstrip line with defected ground structure," *IEE Electron. Lett.*, Vol. 36, No. 21, 1784–1785, Oct. 2000.

13. Shobeyri, M. and M. H. Vadjed-Samiei, "Compact ultra-wideband bandpass filter with defected ground structure," *Progress In Electromagnetics Research Letters*, Vol. 4, 25–31, 2008.

14. Jeong, Y. C. and J. S. Lim, "A novel frequency doubler using feedforward technique and defected ground structure," *IEEE Microw. Wireless Compon. Lett.*, Vol. 14, No. 12, 557–559, Dec. 2004.

15. Song, Q. Y., H. R. Cheng, X. H. Wang, L. Xu, X.-Q. Chen, and X.-W. Shi, "Novel wideband bandpass filter integrating HMSIW with DGS," *Journal of Electromagnetic Waves and Applications*, Vol. 23, No. 14–15, 2031–2040, 2009.

16. Yang, F. R., Y. Qian, and T. Itoh, "A novel uniplanar compact PBG structure and mixer applications," *IEEE MTT-S Digest*, 919–922, Jun. 1999.

17. Radisic, V., Y. Qian, and T. Itoh, "Broad power amplifier using dielectric photonic bandgap structure," *IEEE Microw. Guide Wave Lett.*, Vol. 8, No. 1, 13–14, Jan. 1998.

18. Oraizi, H. and M. S. Esfahlan, "Miniaturization of wilkinson power dividers by using defected ground structures," *Progress In Electromagnetics Research Letters*, Vol. 4, 113–120, 2008.

19. Chang, C.-P., C.-C. Su, S.-H. Hung, Y.-H. Wang, and J.-H. Chen, "A 6 : 1 unequal wilkinson power divider with EBG CPW," *Progress In Electromagnetics Research Letters*, Vol. 8, 151–159, 2009.

20. Lin, C.-M., C.-C. Su, S.-H. Hung, and Y.-H. Wang, "A compact balun based on microstrip EBG cell and interdigital capacitor," *Progress In Electromagnetics Research Letters*, Vol. 12, 111–118, 2009.

21. Fan, F. and Z. Yan, "Dual stopbands ultra-wideband antenna with defected ground structure," *Journal of Electromagnetic Waves and Applications*, Vol. 23, No. 7, 897–904, 2009.

22. Zainud-Deen, S. H., M. E. S. Badr, E. El-Deen, K. H. Awadalla,

and H. A. Sharshar, "Microstrip antenna with defected ground plane structure as a sensor for landmines detection," *Progress In Electromagnetics Research B*, Vol. 4, 27–39, 2008.

23. Hosseini, S. A., Z. Atlasbaf, and K. Forooraghi, "Two new loaded compact palnar ultra-wideband antennas using defected ground structures," *Progress In Electromagnetics Research B*, Vol. 2, 165–176, 2008.

24. Biancotto, C. and P. Record, "Design of a beam forming dielectric cylindrical EBG antenna," *Progress In Electromagnetics Research B*, Vol. 18, 327–346, 2009.

25. Banerjee, A., "Enhanced temperature sensing by using one-dimensional ternary photonic band Gap structures," *Progress In Electromagnetics Research Letters*, Vol. 11, 129–137, 2009.